A&A 672, A165 (2023)
https://doi.org/10.1051/0004-6361/202245593

Astronomy & Astrophysics

Meandering periods and asymmetries in light curves of Miras: Observational evidence for low mass-loss rates⋆

P. Merchan-Benitez[1], S. Uttenthaler[2], and M. Jurado-Vargas[3]

[1] Faculty of Science, University of Extremadura, Avenida de Elvas s/n, 06006 Badajoz, Spain
e-mail: pedromer@hotmail.com
[2] Institute of Applied Physics, TU Wien, Wiedner Hauptstraße 8-10, 1040 Vienna, Austria
e-mail: stefan.uttenthaler@gmail.com
[3] Department of Physics, Faculty of Science, University of Extremadura, Avenida de Elvas s/n, 06006 Badajoz, Spain
e-mail: mjv@unex.es

Received 30 November 2022 / Accepted 30 January 2023

ABSTRACT

Context. Some Miras (long-period variables in late evolutionary stages) have meandering pulsation periods and light-curve asymmetries, the causes of which are still unclear.
Aims. We aim to better understand the origin of meandering periods and light-curve asymmetries by investigating a sample of Miras in the solar neighbourhood. We characterised this group of stars and related their variability characteristics to other stellar parameters.
Methods. We analysed observations from several databases to obtain light curves with maximum time span and temporal coverage for a sample of 548 Miras. We determined their pulsation-period evolution over a time span of many decades, searched for changes in the periods, and determined the amplitude of the period change. We also analysed the Fourier spectra with respect to possible secondary frequency maxima. The sample was divided into two groups with respect to the presence of light-curve asymmetries ('bumps'). Infrared colours and indicators of the third dredge-up were collected to study the mass loss and deep mixing properties of the stars of our sample.
Results. Our analysis reveals one new star, T Lyn, with a continuously changing period. The group of Miras with meandering period changes is exclusively made up of M-type stars. The Fourier spectra of the meandering-period Miras have no prominent additional peaks, suggesting that additional pulsation modes are not the cause of the meandering periods. We confirm that light-curve bumps are more common among S and C Miras and show, for the first time, that Miras with such bumps have lower mass-loss rates than those with regular, symmetric light curves. Also, Miras with meandering period changes have relatively little mass loss.
Conclusions. We conclude that Miras with strongly changing periods (including meandering periods) or asymmetries in their light curves have relatively low dust mass-loss rates. Meandering period changes and light-curve asymmetries could be connected to He-shell flashes and third dredge-up episodes.

Key words. stars: AGB and post-AGB – stars: oscillations – stars: evolution – stars: mass-loss

1. Introduction

Mira stars are long-period variables in the asymptotic giant branch (AGB) phase of stellar evolution. They are characterised by large-amplitude variation ($\Delta V > 2\overset{\text{m}}{.}5$) in their luminosity and pulsation periods of P∼100−1000 d. Most Miras have periods that are stable over time spans of decades or even centuries. Nevertheless, some stars experience significant changes in the pulsation period. Miras with changing pulsation periods were divided into three different groups by Zijlstra & Bedding (2002):

Those that display continuous period changes (CPCs), show a continuous and prolonged increase or decrease in the period over time and no evidence of epochs with stable periods. Only ∼1%−2% of Mira-type variables show CPCs. Highlights are the period changes observed in R Aql, R Hya, and W Dra of $\Delta P/P \sim 15\%$ or more (Wood & Zarro 1981). Miras that exhibit sudden period changes (SPCs) show a sudden and rapid period change after a relatively long phase of stable pulsation period, with a total variation similar to the CPCs but reached in a much shorter time. For example, the period changes observed in T UMi (Gal & Szatmary 1995), R Cen (Hawkins et al. 2001), and RU Vul (Uttenthaler et al. 2016a) are noteworthy. Also this type of period variation is observed in only ∼1%−2% of Mira-type stars. Finally, Miras that show meandering period changes (MPCs) have periods going up and down by up to ∼10% of the average period on timescales of a few decades. The rate of change is comparable to the other two groups, but the total period change is in general slightly smaller than in the other two classes. For example, the variations observed in S Ori amount to ∼9% of its average period (Merchán Benítez & Jurado Vargas 2002). The fraction of observed Mira stars that undergo MPCs is higher than those that undergo CPCs and SPCs, namely of around 10%. This fraction is of the order of 15% if only stars with periods $P > 400$ d are considered.

Several hypotheses have been put forward to explain these period changes. Most importantly, violent ignitions of the He-burning shells called thermal pulses (TPs) are expected to have an important impact on the stellar structure and therefore on the pulsation period of the outer envelope. When a TP sets in, the star shrinks significantly, and its pulsation period shortens. As this is predicted to happen within a few decades, it is thought that the onset of a TP may explain the SPC class of Miras with strongly decreasing periods. From theoretical

⋆ Full Table B.1 is only available at the CDS via anonymous ftp to cdsarc.cds.unistra.fr (130.79.128.5) or via https://cdsarc.cds.unistra.fr/viz-bin/cat/J/A+A/672/A165

considerations (Wood & Zarro 1981), it is expected that ∼1% of Miras undergo this phase in the TP cycle at any one time. At later phases of the TP cycle, the changes in stellar radius and therefore pulsation period become slower, and so the CPC class of Miras may also be explained as a result of a TP.

From an observational point of view, stars undergoing TPs can be distinguished based on nucleosynthesis products such as radioactive technetium (Tc) and ^{12}C mixed to the stellar surface in deep-mixing events called the third dredge-up (3DUP). A 3DUP event may occur several hundred years after the TP ignition (Herwig 2005), and Tc can be detected in optical stellar spectra (Little et al. 1987; Uttenthaler et al. 2011). However, the absence of Tc does not necessarily mean the absence of TPs because they may not yet have become powerful enough to drive 3DUP in their aftermath.

Templeton et al. (2005) analysed decades-long light curves of Mira-type variables, finding that only ∼10% showed significant period variations on timescales of decades. Among them, only eight (∼1.6%) showed highly significant monotonic period changes, a fraction consistent with that expected for stars in the early post-TP phase, where the models predict the largest period change. The rest of the stars with significant but non-monotonic period changes belong to the MPC group in the Zijlstra & Bedding (2002) classification.

The physical mechanism to account for these MPCs is unclear, but various theories have been put forward in recent decades. Templeton et al. (2005) speculate that MPCs might also be related to TPs, although the timescales of these variations (several decades) are much shorter than those predicted for global changes induced directly by a TP. Ostlie & Cox (1986) worked with several AGB model stars in the mass range of 0.8−2.0 $M_{\odot}$ and obtained Kelvin-Helmholtz cooling timescales $\tau_{\rm KH}$ of between 6 and 200 yr. The timescales observed in the MPCs are therefore similar to the Kelvin-Helmholtz cooling timescale of the envelopes of solar-like stars. Therefore, these shorter period variations may be thermal relaxation oscillations in response to the global changes caused by a TP. Another explanation, in this case non-evolutionary, is that the pulsations of Mira variables are intrinsically non-linear by nature and exhibit low-dimensional chaotic behaviour (Kiss & Szatmáry 2002). Amplitude (not period) variations in the light curve of some of these stars could be due to the non-linear interaction of two or more pulsation modes, which is similar to what is found for RV Tauri stars (Buchler et al. 1996). Another hypothesis is that the pulsations of Mira-type variables may be strong enough to modify the stars' internal structure (Ya'Ari & Tuchman 1996); they could modify the entropic structure of the star over time, causing both a change in pulsation mode and a readjustment of the equilibrium structure.

The shapes of the light curves of Mira variables have also been studied. Here, the presence of asymmetries such as so-called 'bumps' or 'humps' are of particular interest. Classification systems of Mira light curves have, for example, been established by Campbell (1925) and Ludendorff (1928). The latter separated the stars into three main groups (α, β, and γ) and further divided them into a total of ten subgroups. Vardya (1988) included an asymmetry factor f in the classification, defined as the rise time in proportion to the mean pulsation period, and found that only a fraction of ∼20% of the Miras shows substantial deviations from a symmetric light curve with $f \leqslant 0.4$ or $0.5 \leqslant f$. Lebzelter (2011) used the parameter χ^2, which is defined as the sum of the squared differences between the light curve of a star and a sinusoidal reference curve, and found that ∼30% of the sample stars have light curves that significantly deviate from a purely sinusoidal shape. Lebzelter also found a connection between atmospheric chemistry and light-curve shape, with a higher fraction of S and C stars with non-sinusoidal variations compared to M stars. However, no simple correlation between light-curve shape and various colour indices was found. On the other hand, Lockwood & Wing (1971) found that the stars' spectral types change along the rising and descending branches, but they do not appear to be directly related to the asymmetries and bumps observed. These authors determined that the stellar temperature increases continuously from minimum to maximum light regardless of whether or not there are bumps. In summary, no clear explanation for light-curve asymmetries exists to date.

Several papers have focused on CPC and SPC stars, but there have been very few systematic studies on MPC stars. In this paper, we analyse the periods and light curves of a sizeable sample of Miras in the solar neighbourhood, focusing on the MPC class to shed more light on the origin of this type of period change. We search multi-decade light curves for period changes, quantify the amplitude of period change, and inspect information on the 3DUP activity and mass loss of the sample stars. The mass-loss properties of Miras with changing pulsation periods, particularly the MPC group, have received very little attention in the literature, with a few exceptions (Zijlstra et al. 2002).

2. Sample stars and data reduction

2.1. Sample selection and data collection

We used the long-term observations collected in four databases to search for period changes: AAVSO (American Association of Variable Star Observers), AFOEV (French Association of Variable Star Observers), ASAS (All Sky Automated Survey), and DASCH (Digital Access to a Sky Century at Harvard). Most data are visual or V-band observations of the AAVSO and AFOEV. In these two databases, the visual observations are heterogeneous because they are made by a large number of observers with slightly different ocular responses and observing methods; they are therefore subsequently subjected to an averaging process, which we describe below. On the other hand, the large amount of observational data collected allows us to obtain long-term average light curves with good accuracy, reaching, in some cases, more than 120 yr of observation. The V-band photometric data collected from the ASAS database stem from observations obtained by a CCD photometric tracking program at Las Campanas Observatory, Chile, in the declination range −90° to +28° between 2000 and 2009. The limiting magnitude is about $14\overset{\rm m}{.}5$, and about 500 observations per star have been collected. Finally, the historical data in the DASCH database come from an archive of digitised photographic plates of the Harvard College Observatory (Laycock et al. 2010) dating back several decades to over 100 yr. However, the temporal coverage of the ASAS and DASCH databases alone is too low to analyse the long-term period evolution. The ASAS database covers intervals of about ten years, while in the DASCH database, we can find very old observations but generally very dispersed in time. Therefore, although they are a great tool to use in combination with the other databases, they alone do not usually allow a detailed study of the period changes.

In addition, we used the relatively short-term, high-cadence ASAS-SN (All-Sky Automated Survey for Supernovae, Shappee et al. 2014) Catalog of Variable Stars III (Jayasinghe et al. 2019) to analyse light-curve shapes and search for asymmetries (Sect. 3.3). For the stars with insufficient

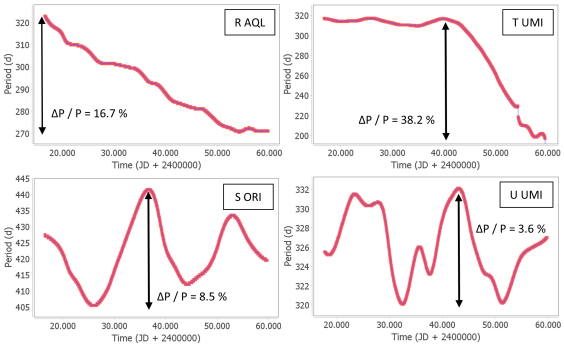

Fig. 1. Typical examples of period changes found with the VStar program: *Top left:* continuous period change (R Aql); *Top right:* sudden period change (T UMi); *Bottom left:* significant meandering period change (S Ori); *Bottom right:* non-significant meandering period change (U UMi).

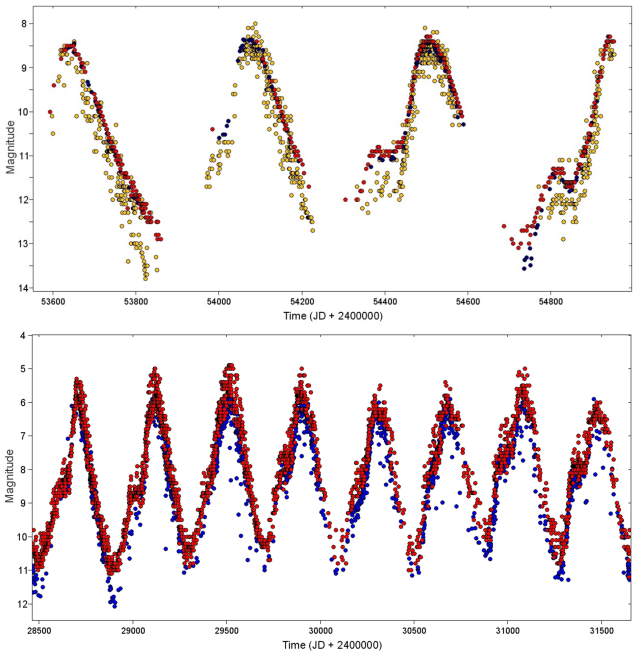

Fig. 2. Combined individual data from different databases. *Top panel:* S Ori: visual AAVSO (yellow), *V*-band AAVSO (blue), and ASAS (red). *Bottom panel:* T Cep: visual AAVSO (red) and DASCH (blue).

ASAS-SN observations or those with poorly covered rising branches of the light curve, we turned to *V*-band photometric data from the AAVSO database and ultimately to binned light curves as described in Sect. 2.2.

We began by reviewing the variables marked as Mira type in the General Catalog of Variable Stars (GCVS, Samus' et al. 2017), where we found around 8000 stars. Of these, we discarded those with a full *V*-band amplitude of less than $2^{\rm m}.5$ (i.e. those stars not fulfilling the amplitude criterion of Miras), obtaining a first selection of about 1500 Mira-type variables. Many of these stars are very faint, and so their light curves in the AAVSO and AFOEV databases are too sparse to analyse the period evolution. We therefore eliminated these from our selection by a simple visual inspection of their light curves. Based on these criteria, our final selection contains 548 Mira-type variables, of which 472 are M-type, 43 are S-type, and 33 are C-type. Although our sample size is almost identical to that of Templeton et al. (2005, 547 stars), we have only 465 stars in common. The largest part of the difference may be explained by the fact that our time series are augmented by DASCH data where possible, and our selection criteria do not include stars such as semi-regular variables or symbiotics.

In these 548 sample stars, we studied the period changes using the VStar program, which includes the option of performing a time-frequency analysis through the weighted wavelet z-transform (WWZ; Foster 1996). With this tool, we constructed plots of the period versus time and determined the full amplitude of period variations, calculated as the ratio between the observed amplitude of the period variation and the mean period obtained by Fourier analysis of the complete data. We then separated the sample stars with large period changes into the three groups described in Sect. 1: stars with continuous (CPCs), sudden (SPCs), and meandering (MPCs) period changes. Figure 1 shows typical examples of these different types of period changes in a period vs. time plot. This figure includes two examples of MPCs: S Ori as one of the most obvious examples of a Mira with a period change of greater than 5% (which we refer to below as significant MPC; see Sect. 4.1), and U UMi, with a period change of less than 5%. Figure 1 also illustrates the definition of the full amplitude of period variation calculated for each star.

2.2. Binning and averaging light curves

We focus on those Mira-type variables among the 548 sample stars that present either significant meandering period changes above 5% or clear asymmetries or bumps in their light curves. For these latter stars, we collected all available data in the four databases, seeking the maximum temporal coverage to analyse their period changes and as much data as possible to analyse in detail the shape of their light curves (e.g., bumps). All these observations were subjected to a validation process during which discrepant data or data with high uncertainty were eliminated. Subsequently, we checked in the graphs whether or not they could be combined. As an example, Fig. 2 shows sections of the light curves of S Ori and T Cep with all the data combined, where we can observe that the minor differences that may exist between the various databases do not exceed the dispersion level of the data. Therefore, data from all sources were merged to calculate the average light curves.

For the averaging process of the observations, we tailored a code to calculate the average value of all the individual data with intervals of between 3 and 5 days, depending on the pulsation period of the star, obtaining between 70 and 80 data points per cycle. Double weight was assigned to the AAVSO, AFOEV, ASAS, and DASCH *V*-band photometric data compared to the AAVSO and AFOEV visual data because of the higher precision of the former. The result can be seen in Fig. 3, which shows the final processed light curve of T Cep as an example. The plots demonstrate that our binning and averaging process results in very smooth light curves that are well suited for further analysis.

2.3. Frequency test

To determine the possible impact of the binning process and subsequent averaging of data on the Fourier spectra, as well as to study the possible appearance of artificial peaks, we performed two different tests, as in Kiss et al. (1999). In the first test, we compared the Fourier spectrum of the raw data with that of the averaged data in five-day bins. The results of this test are shown in Fig. 4 for T Cep and T Cas. These two stars were chosen because the number of observations differs significantly: 121 622

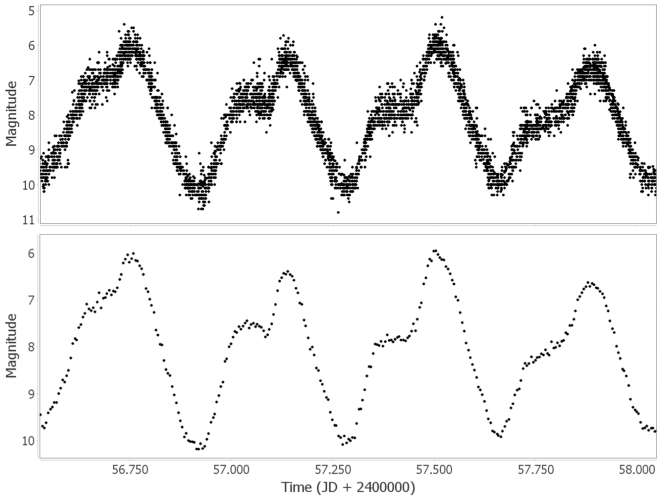

Fig. 3. Section of the light curve of T Cep. *Top panel:* raw observational data. *Bottom panel:* final data after processing and averaging in five-day bins.

and 55 417, respectively. The dominant frequency obtained is shown in the figure. No additional peaks appear, and the main frequency remains almost unchanged in both position and amplitude. The structure of the main peaks is preserved, and the aliasing peaks diminish. Similar results were obtained by performing this process with the rest of the stars analysed in this study.

The second test was done with synthetic light curves and pursued two aims: (i) to check the impact of seasonal observation gaps on the appearance of additional peaks in the Fourier spectrum, and (ii) to check whether or not our analysis program can recover the phases of period increase or decrease similar to those observed in MPC stars. We generated several synthetic light curves with random observational noise to the magnitude (Gaussian noise with $\sigma = 0\overset{\mathrm{m}}{.}15$) and the observation date (uniformly distributed shifts of ±2 d to the five-day bins). The synthetic light curves span a time of about 65 yr. With these artificial data, we tried to mimic the observations used for the analyses and the period changes observed in the MPC stars, both in depth (between 5% and 10%) and in timescale (several decades). These synthetic light curves were generated in two different situations. First, a continuous period increase of 10% was assumed (between 400 and 440 days over about 25 yr), including 20 yr of constant period before and after the increase. The second situation assumed a continuous period decrease of 5% (between 525 and 500 days over 25 yr) and stable period phases of about 20 yr before and after. In addition, in both situations, we varied the length of the seasonal gaps between approximately 0, 30, 60, and 90 days. The left panel of Fig. 5 shows the case results corresponding to a continuous period increase of approximately 10% with seasonal gaps of 90 days; this verifies that the result is in good agreement with the input parameters.

We also analysed a synthetic light curve containing phases of rising and falling periods. The Fourier spectrum of this light curve shows a broad peak between the frequencies corresponding to the minimum and maximum period but without additional peaks beyond those corresponding to the seasonal aliases. Period-versus-time plots clearly reveal the evolution of the input period (right panel of Fig. 5). Therefore, we conclude that our analysis program can reliably recover the actual period changes in the observed stars and allows us to interpret the possible peaks appearing in the Fourier analyses.

2.4. Additional data

As we aim to study the mass-loss properties of our stars, we need a measure of their mass-loss rates. The best (gas) mass-loss rates are traditionally determined from radio CO rotational lines. However, they are available only for a small fraction of our sample stars. Therefore, we mainly use the $K - [22]$ colour as an indicator of the dust mass-loss rate. Although this infrared (IR) colour traces only the dust in the stellar outflow, which is a small fraction of the total mass loss, and the dust-to-gas ratio in the outflow is suspected to vary from star to star, McDonald et al. (2018, see their Fig. 5) showed that this is directly related to the total (gas) mass-loss rate above a cut-off of $K - [22] > 0\overset{\mathrm{m}}{.}55$. Throughout this paper, we refer to the mass-loss rates of the stars, but keep in mind that the IR colours are only indicators of the dust mass-loss rate. We collected photometric data to calculate colour indices such as $K - [22]$ and $[3.4]-[22]$. The K-band magnitude was taken from the 2MASS catalogue (Skrutskie et al. 2006) or, when available, from the compilation of average magnitudes in Uttenthaler et al. (2019). The [3.4] and [22] magnitudes were measured by the Wide-field Infrared Survey Explorer (WISE) space observatory (Wright et al. 2010) and are taken from the AllWISE (Cutri et al. 2021) or, in case of saturation, from the unWISE catalogue (Schlafly et al. 2019).

Furthermore, information about technetium (Tc) and the carbon isotopic ratio was collected in order to inspect the 3DUP activity of our sample stars. Tc data were adopted from Little et al. (1987), Uttenthaler et al. (2019, and in prep.). Literature sources for the $^{12}C/^{13}C$ comprised of Lambert et al. (1986), Ohnaka & Tsuji (1996), Abia & Isern (1997), and Greaves & Holland (1997) for the C-type stars; Dominy & Wallerstein (1987), Schöier & Olofsson (2000), and Lebzelter et al. (2019) for S-type stars; and Ramstedt & Olofsson (2014) and Hinkle et al. (2016) for M-type stars.

Infrared colour indices are available for all stars, Tc observations for 154 stars, and $^{12}C/^{13}C$ ratios for 47 stars. All data are listed in Table B.1.

3. Period changes and light-curve shapes

3.1. The stars with the strongest period changes

We derived relative period changes $\Delta P/\langle P\rangle$ for the 548 stars of our sample. Here, ΔP is the full amplitude of the period change, and $\langle P\rangle$ is the mean period obtained by our Fourier analysis of the complete time series available. The quantity $\Delta P/\langle P\rangle$ should be better suited to identifying MPC Miras than a linear fit to the period evolution, as used for example by Templeton et al. (2005). We verified that $\Delta P/\langle P\rangle$ is essentially independent of the length of the available time series. However, we cannot exclude that the relative period change might be underestimated for the shortest time series in the sample ($\lesssim$20 000 d, equivalent to ~55 yr). Applying a limit of variation of $\Delta P/\langle P\rangle > 5\%$ (roughly equivalent to the $2-3\,\sigma$ significance level of Templeton et al. 2005), we find a total of 27 Mira variables that surpass this limit; their data are shown in Table 1. Column 4 of this table contains the period change over the analysed time. Our choice of the 5% limit is justified below in Sect. 4.1.

Five Miras are classified as CPC, namely R Aql, W Dra, R Hya, T Lyn, and Z Tau, and four as SPCs, namely R Cen, BH Cru, LX Cyg, and T UMi. These nine stars account for

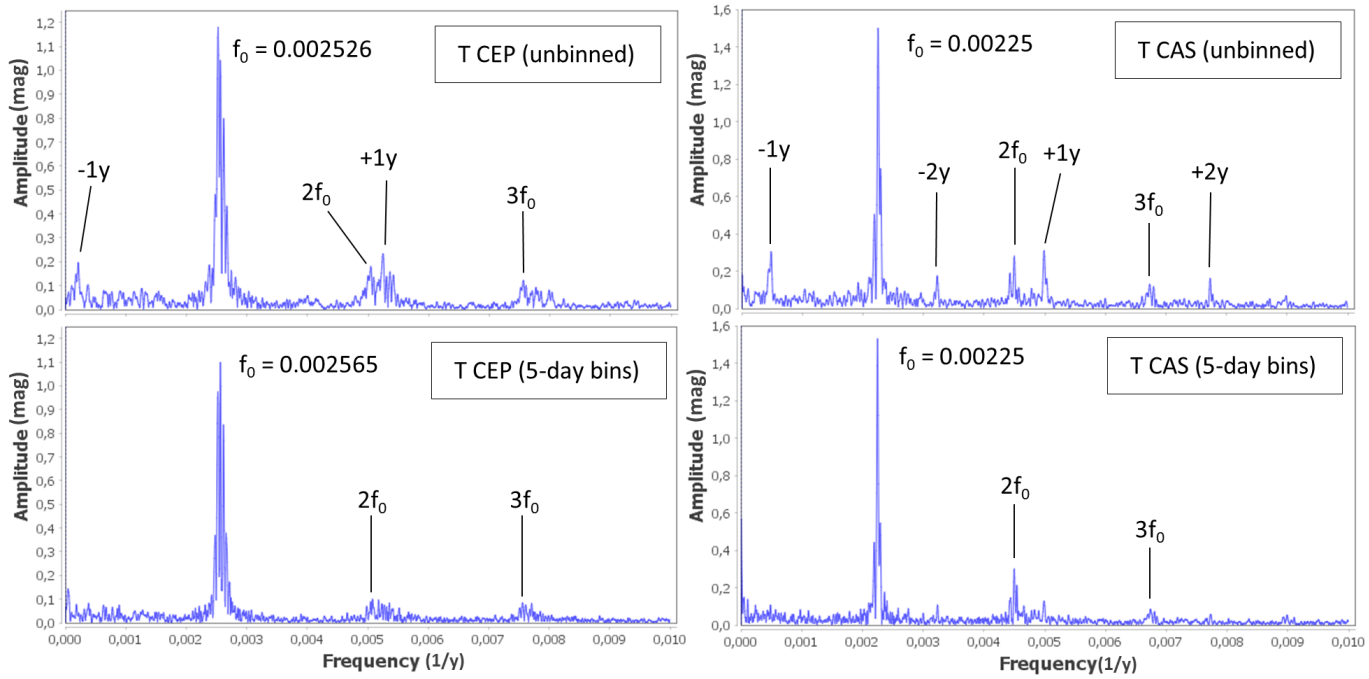

Fig. 4. Fourier spectra of T Cep and T Cas using unbinned data and five-day binning; see figure legend.

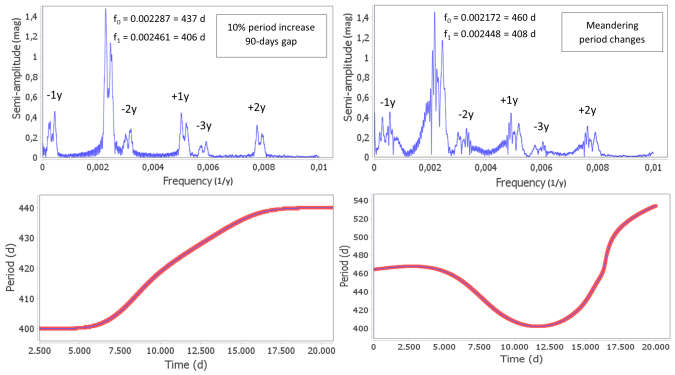

Fig. 5. Numerical tests with synthetic light curves. *Left panels:* continuous period increase of approximately 10%, with seasonal gaps of 90 days. *Right panels:* alternating period decrease and increase, simulating MPC-type variations.

~1.6% of the total sample, which agrees well with the fraction of stars with highly significant period changes obtained by Templeton et al. (2005). The only difference between this latter study and ours lies in the carbon Mira T Lyn, for which we find a period change of 6.4%, which happened relatively continuously. As we can see in Fig. 6, half of the period change in T Lyn occurred in the last 15 yr or so, which is probably why it did not appear among the most significant period changes in the survey of Templeton et al. (2005) almost 20 yr ago. We therefore propose T Lyn as a new CPC candidate and recommend monitoring its period evolution.

We also highlight the case of BH Cru: Prior to 1999, it experienced an increase of about 25% relative to the average period given in the GCVS (1970). On the other hand, we detected a period decrease of 9.5% since 1999. It has been speculated that the period increase in BH Cru (and LX Cyg) is the result of a recent 3DUP event in the aftermath of a TP that increased its atmospheric C/O ratio from ~1 to >1 (Whitelock 1999; Uttenthaler et al. 2016b). The increased C/O probably provides feedback to the pulsation mechanism because of higher atmospheric opacity. Possibly, the maximum period reached after this event is not long-term stable. BH Cru is an exciting object to study in depth, and we recommend monitoring its period evolution.

The group of 18 MPC Miras in Table 1 is exclusively made up of M-type stars. Based on the distribution of the spectral types in the sample (472 M-type, 43 S-type, 33 C-type), basic combinatorial considerations yield a probability of ~6.6% to draw only M-type stars when randomly selecting 18 from the sample. Though it cannot be excluded that this is a chance result, it seems plausible that significant MPCs are much more common among M-type Miras than among the other spectral types. Figure A.1 presents the result of the period evolution analysis carried out with the VStar program for these 18 MCP candidate stars. It shows the period versus time and period versus time versus WWZ 2D contour plots for all of them. We can read off from these diagrams that the period meanders with typical timescales of 30–75 yr.

Interestingly, the distribution of period variations $\Delta P/\langle P\rangle$ does not peak around zero, that is, a completely stable period is not the most common property. Instead, the distribution shows a peak at ~2%; the median value is 2.4%. This would also be the precision to which pulsation periods of Miras can be determined in general, which also affects the width of period–magnitude relations of Miras (Soszynski et al. 2007).

3.2. Fourier analysis of Mira stars with significant MPCs

Fourier analysis of stellar light curves can reveal important information about how brightness variations occur. It is often a complex process because the discrete Fourier transform (DFT) can introduce additional misleading frequencies due to cycle-to-cycle variations, long-term brightness changes, gaps in the light curves, and so on, in addition to the non-constant periods

Table 1. Mira-type stars with significant period changes.

GCVS	$\langle P \rangle$ [d]	Spectral type	$\Delta P/\langle P \rangle$ %	$K - [22]$ [mag]
MPC				
RU Tau	588.6	M3.5e-M6.5	9.5	1.685
S Ori	409.2	M6.5e-M9.5e	8.5	1.733
RS Aql	417.9	M5e-M8	7.2	2.531
U CMi	411.6	M4e	7.0	2.018
T Cep	390.2	M5-M9IIIe	7.0	1.246
Z Vel	411.4	M9e	7.0	2.327
T Hya	285.7	M3e-M9:e	6.7	1.351
RU Sco	370.5	M4/6e-M7II-IIIe	6.7	2.142
T CMi	316.2	M4Se-M8	6.5	1.867
AF Car	446.5	M8e	6.3	1.889
S Sex	259.0	M2e-M5e	6.0	1.704
T Ser	340.0	M7e	5.9	1.567
W Lac	320.2	M7e-M8e	5.8	1.955
SU Her	341.6	M6e	5.7	1.963
SS Peg	416.3	M6e-M7e	5.7	1.962
S Her	305.5	M4.Se-M7.5,Se	5.2	1.032
TY Cyg	357.0	M6e-M8e	5.1	1.868
Z Sco	345.3	M5.5e:-M7e	5.0	1.633
CPC				
R Aql	280.7	M5e-M9IIIe	16.7	2.270
R Hya	388.0	M6e-M9eS	15.4	0.839
W Dra	279.3	M3e-M4e	14.9	3.033
Z Tau	458.5	S7.5,1e(M7e)	11.8	2.633
T Lyn	409.0	C5.2e-C7.1e	6.4	2.148
SPC				
T UMi	317.3	M4e-M6e	38.2	1.212
LX Cyg	477.0	C(N)	22.6	1.602
R Cen	571.5	M4e-M9.5	13.9	2.163
BH Cru	528.7	C(N)	9.5	1.573

Notes. The stars are grouped in MPC, CPC, and SPC classes. Column 1: Denomination in GCVS; Col. 2: Mean period obtained by Fourier analysis of the time series data; Col. 3: Spectral type in GCVS; Col. 4: Relative period change; Col. 5: $K - [22]$ colour.

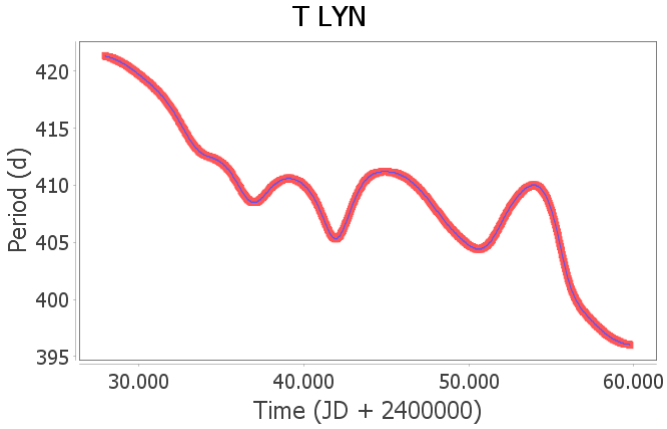

Fig. 6. Period evolution of the carbon Mira T Lyn. A strong period decrease commenced about 15 yr ago, continuing the trend seen at the beginning of the available time series.

of MPC stars. As observed in Sect. 2.3, the Fourier spectrum shape of MPC stars is dominated by a structure of peaks around the primary frequency (f_0) accompanied by its harmonics ($2f_0, 3f_0, \ldots$). Moreover, as the time series are not homogeneous and have gaps, seasonal aliases ($\pm$1y, $\pm$2y, ...) appear. In a few cases, the time series are almost uninterrupted, with only one seasonal alias appearing. Finally, due to a physiological effect called the Cerasky effect, the visual observations may additionally have a spurious period of about one year (f_y) (see for these topics e.g., Kiss et al. 1999; Templeton et al. 2005; Percy 2015).

We calculated the Fourier spectra of the 18 MPC stars using the Fourier routine DC-DFT in the AAVSO software package VStar. We then analysed the structure of the frequency peaks in a semi-amplitude versus frequency diagram. The data were merged, separated into bins, and averaged according to the process described in Sect. 2.2. In cases where the number of data points is low and gaps are very frequent, the level of background noise makes it difficult to identify peaks, and so power versus frequency plots were used to highlight the dominant frequencies. Figure 7 shows the Fourier spectra and the identification of obvious peaks for three stars with different characteristics in the collected data. The top panel shows T Cep, with the highest number of data points and an almost uninterrupted time series, and so only one seasonal aliasing is minimally noticeable in addition to the primary frequency and its first two harmonics. The middle panel shows the Fourier spectrum of S Ori, a star with a much smaller number of data points and seasonal gaps. This star displays a more complex structure of seasonal aliases in addition to its first harmonics. The appearance of the seasonal frequency f_y can also be seen. The lower panel of Fig. 7 shows the spectrum of AF Car, the star with the fewest and most scattered data points. For this object we had to resort to the power versus frequency plot with a smoother noise background. Nevertheless, it can be seen that, besides only a faint unidentified peak f_1 with a power of ~10% that of f_0, no obvious peaks appear in AF Car's spectrum beyond those discussed above.

Figure A.1 shows the same analysis for the remaining 15 stars, and we can see that none of these Fourier spectra show prominent additional peaks. Along with AF Car mentioned above, there are only three other stars (RU Sco, RS Aql, and SS Peg) with some unidentified frequency peaks, marked as f_1, but with low amplitude.

3.3. Light-curve shapes

We are interested in the light curves of our sample stars because we find that 16 out of the 18 stars with significant MPCs (Table 1) have apparent bumps on the ascending branch of most light cycles. For the remaining two stars, W Lac and Z Sco, we cannot state with certainty the presence of bumps because of the relatively low number of observations in the ascending branch of their cycles. We visually inspected the ASAS-SN light curves and phase diagrams and qualitatively divided all sample stars into two large groups:

Group A (asymmetric). These are stars with apparent asymmetries in their light curves, such as bumps on the rising branch, double maxima, or abrupt changes in the slope of the rising branch. Given the similarity of all these anomalies, they may correspond to a larger or smaller-scale expression of similar phenomena in the stars' atmospheres and represent a relatively homogeneous group. We find a total of 203 Mira-type variable stars with these characteristics. This fraction of 203/548 $\approx$ 37% is slightly higher but in relatively good agreement with the findings of previous studies, namely Vardya (1988, 20%) and

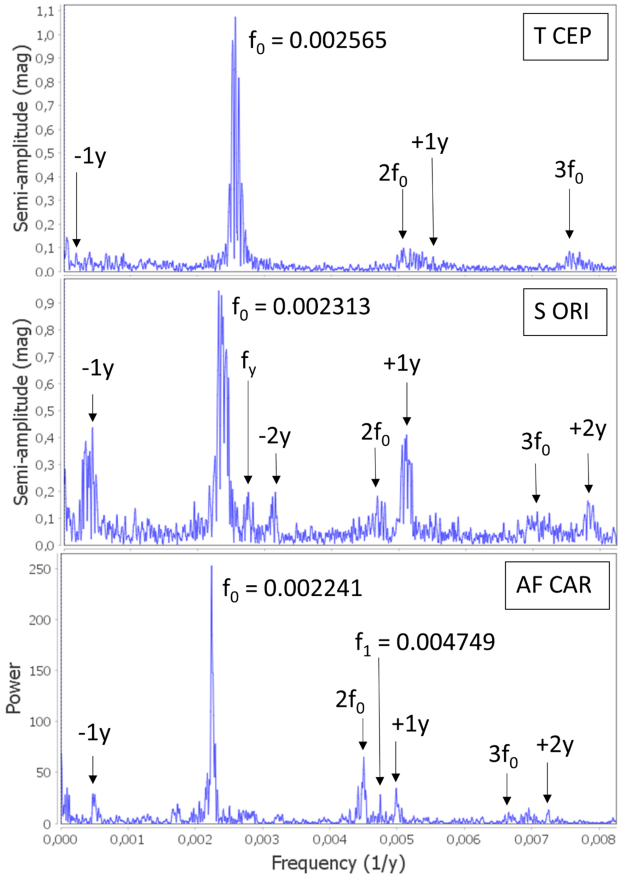

Fig. 7. Fourier spectra and identification of frequency peaks of three Miras with significant MPCs. Besides the harmonics of the main frequency and seasonal aliases, no obvious additional peaks appear in the spectra.

Lebzelter (2011, 30%). Group A would include the stars that Ludendorff (1928) classified as γ-type stars.

Group S (symmetric). This group includes the remainder of the sample, that is the 336 stars without anomalies in the rising branch of their light curves. This also includes doubtful cases in which the possible observed anomalies occur only in a few cycles or are so weak that we cannot be certain of their existence. Although this aspect may introduce some uncertainty in our results, the high number of stars in our selection and the use of up to four different sources to inspect the light curves minimises these uncertainties. This group would correspond to the α- and β-type stars of the Ludendorff classification.

Given this procedure to classify stars in Group A only if they have evident anomalies, we expect Group A to be relatively pure. In contrast, Group S might contain a few stars that would be classified as Group A had better data been available. In Fig. 8, we show example light curves of Miras in Group A (left columns) and light curves of Miras in Group S (right columns). Figure 3 shows a portion of the light curve of T Cep, another example of a Mira in Group A. Table B.1 collects the classification with respect to light-curve asymmetries.

3.4. 3DUP indicators

Thermal pulses and 3DUP events have been proposed as the basis of the various period change classes. If this is the case, one would expect these stars to show the 3DUP indicator Tc in their spectra and have increased $^{12}C/^{13}C$ ratios. Table 2 shows the data of the stars with significant period changes from Table 1 for which information about Tc is available. We found information for only 5 of the 18 stars with significant MPCs in our sample; in 4 of which the presence of Tc has been confirmed, or Tc is likely present. We reiterate the fact that the absence of Tc does not necessarily mean the absence of TPs because they may have yet to become powerful enough to drive 3DUP in their aftermath. Nevertheless, it seems likely that many of them have indeed undergone 3DUP events. Further observations are required in order to come to a more robust conclusion.

The distribution of the 203 Group A stars in terms of their spectral types has an interesting pattern. Stars with bumps in their light curves are much more common among S- and C-type than among M-type stars. Specifically, the fraction is $32/40 \approx 80\%$ for the S-type, $24/32 \approx 75\%$ for the C-type, and only $147/467 \approx 31\%$ for the M-type Miras. This is in agreement with the result of Lebzelter (2011), who find that S and C stars generally show a higher fraction of non-sinusoidal variation than the M-type stars. The higher C/O ratio of more advanced evolutionary stages might favour the presence of asymmetries in the light curves.

This suggests that there could also be a relation between light-curve shape and 3DUP activity. All S- and C-type sample stars observed for Tc are confirmed to be Tc-rich, and many also have bumps. The histogram of how the M-type stars in the two groups are distributed with respect to the presence of Tc in their spectra is displayed in Fig. 9. The classifications 'doubtful' (dbfl), 'possibly' (poss), and 'probably' (prob) are used only in Little et al. (1987), which we retain here. Restricting the selection to the unambiguous 'yes' and 'no' classifications of Uttenthaler et al. (2019), we find 17 Tc-poor and 18 Tc-rich M-type Miras in Group A. On the other hand, there are 37 Tc-poor M-type stars in Group S, but only one Tc-rich star. Thus, while Group A contains many Tc-rich stars of all spectral types, Group S is almost devoid of Tc-rich ones. We therefore conclude that, given the prior condition that a Mira of any spectral type is Tc-rich, the probability that it also has bumps in its light curve is of the order of $(18+32+24)/(19+40+32) = 81.3\%$. On the other hand, given the prior condition that an M-type Mira has no bumps, the probability that it is Tc-poor is almost 100%.

We can also check on the population level whether or not the fractions of Miras with light-curve asymmetries and with the 3DUP indicator Tc agree. If these things are connected somehow, the respective fractions should be similar. We better avoid selection biases that could plague especially the Tc observations collected from many literature sources and therefore focus on the M-type Miras. M-type Group A stars in the complete sample make up a fraction of $147/467 = 0.315$. On the other hand, M/MS-type Galactic-disc Miras with Tc in the sample of Uttenthaler et al. (2019) make up a fraction of $28/105 = 0.267$. Given a base fraction of 0.315, the probability of drawing 28 or fewer Tc-rich stars out of 105 M-type stars is 17%. Therefore, we cannot reject the notion that the two fractions are identical with high confidence.

In addition to Tc, the carbon isotopic ratio $^{12}C/^{13}C$ is an indicator of the 3DUP activity of an AGB star. When the first TP takes place on the AGB, the $^{12}C/^{13}C$ ratio is expected to be of the order $10 \lesssim {}^{12}C/^{13}C \lesssim 25$, depending on the initial mass (Hinkle et al. 2016). The lowest values, $10 \lesssim {}^{12}C/^{13}C \lesssim 20$, would be found in stars with masses $\lesssim 2\,M_{\odot}$, while the highest values, $20 \lesssim {}^{12}C/^{13}C \lesssim 25$, would be found in the most massive stars. For stars undergoing 3DUP episodes, the carbon

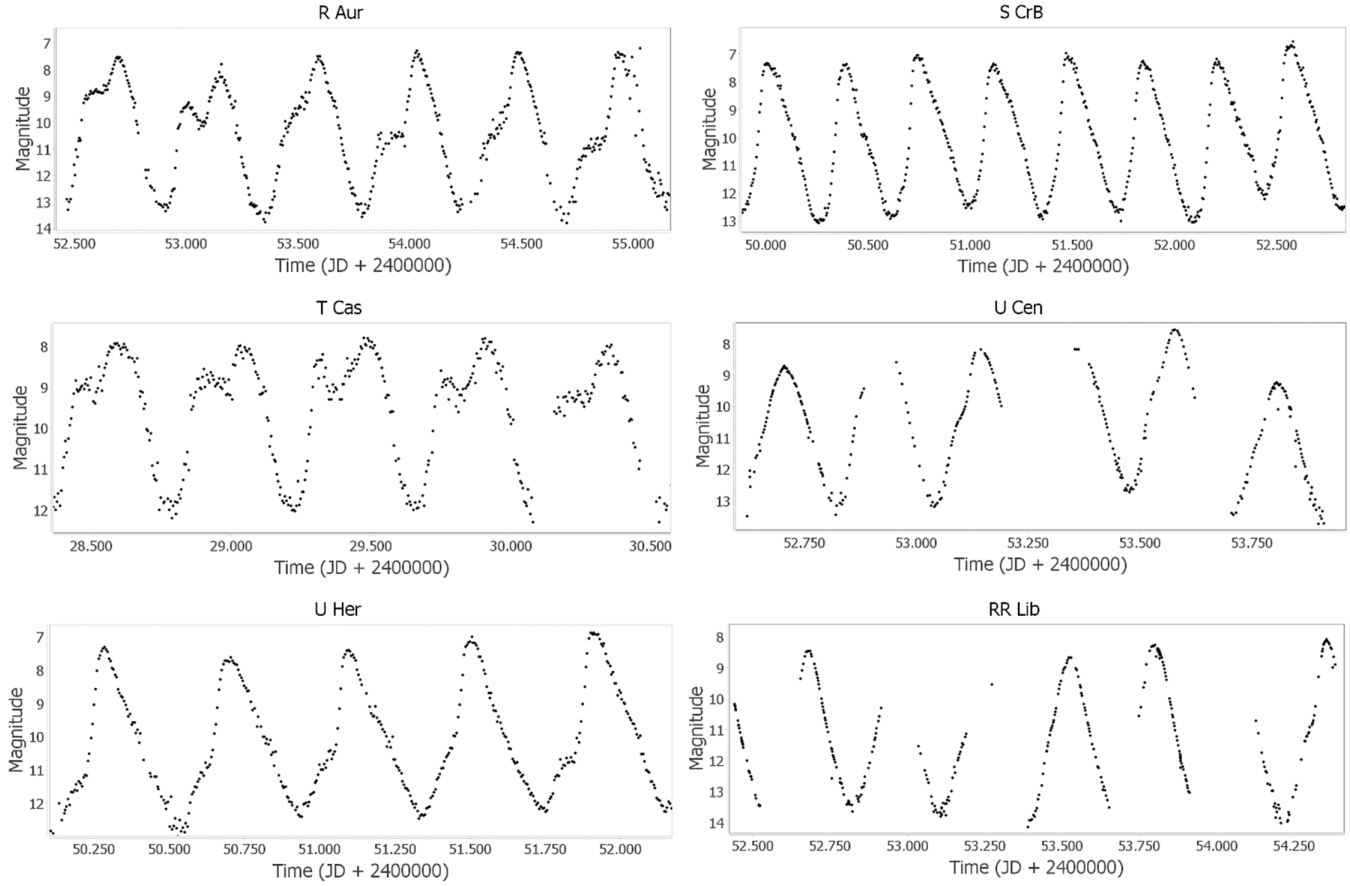

Fig. 8. Example light curves of Groups A and S stars. *Left column:* Group A. From top to bottom: R Aur (bumps in the ascending branch), T Cas (double-peaked maximum), and U Her (abrupt change in the slope of the ascending branch). *Right column:* Group S. From top to bottom: S CrB (quasi-sinusoidal light curve), U Cen (slight asymmetries only in some of its cycles), and RR Lib (gaps in the light curve prevent us from identifying asymmetries with certainty).

isotopic ratio will increase as new ^{12}C synthesised in the He-burning layer is brought to the surface. We may therefore identify M-type Miras that underwent 3DUP events by their carbon isotopic ratio elevated to values of $^{12}C/^{13}C \gtrsim 25$.

Among the 47 sample stars for which we find $^{12}C/^{13}C$ isotope ratios in the literature (Sect. 2.4), 23 are M-type, 10 are S-type, and 14 are C-type. The $^{12}C/^{13}C$ is known for two M-type stars with significant MPCs in our sample, S Ori and T Cep. The values are reported to be 45 ± 10 and 33 ± 10, in agreement with the fact that both are also Tc-rich. Even the next two stars with non-significant MPCs but with relatively high $\Delta P/\langle P\rangle$ values with known isotopic ratios, RU Her and R Aur with $\Delta P/\langle P\rangle$ of 4.5 and 4.4, have $^{12}C/^{13}C$ values of 25 and 33, respectively. This agrees with the fact that they are also reported to contain Tc.

The few carbon isotopic ratios available in the literature support the findings from Tc concerning the light-curve shapes. The $^{12}C/^{13}C$ ratio is reported for four stars from Group S: Two classified for Tc as 'doubtful' and 'no' have ratios of 12 and 16, and two Tc-rich ones have ratios of 22 and 26. Also, the carbon isotopic ratios of Group A stars agree with their Tc classifications: The mean $^{12}C/^{13}C$ of the nine Tc-poor stars is 13 (range 8−19), and that of the seven Tc-rich is 28 (range 14−45). Among the 29 M-type Miras we have in common with Hinkle et al. (2016), 9 have $^{12}C/^{13}C \geq 25$ (taking into account the measurement uncertainty), indicating the possibility of having undergone ^{12}C enrichment by 3DUP events. Indeed, the literature confirms that most of them also have Tc in their atmosphere, or at least Tc is possibly or probably present. Interestingly, all nine stars are in our Group A of stars with bumps in the ascending branch of their light curves. The data for these stars were extracted from Table B.1 and are shown separately in Table 3. This underlines the possibility of a connection between bumps in the light curve and the occurrence of 3DUP events.

Table 2. Tc information for stars with significant period changes.

GCVS	Tc	GCVS	Tc	GCVS	Tc
MPC		CPC		SPC	
S Ori	yes (1)	R Aql	no (1)	T UMi	no (1)
U CMi	no (2)	R Hya	yes (1)	LX Cyg	yes (1)
T Cep	yes (1)	W Dra	no (1)	R Cen	no (1)
T Hya	prob (2)			BH Cru	yes (1)
S Her	yes (1)				

Notes. (1): Uttenthaler et al. (2019); (2): Little et al. (1987).

4. Mass-loss properties

4.1. Mass loss as a function of relative period change

To connect the period variations presented above to colour indices and mass-loss considerations, it is first insightful to plot

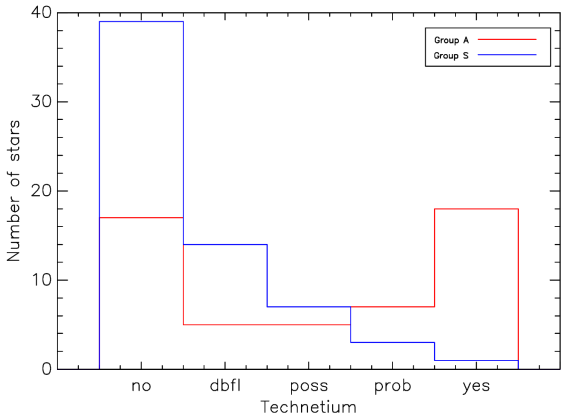

Fig. 9. Distributions of M-type stars in Groups A and S with respect to the presence of Tc. The classifications 'doubtful' (dbfl), 'possibly' (poss), and 'probably' (prob) are used only in Little et al. (1987), whereas 'no' and 'yes' are used by both Little et al. (1987) and Uttenthaler et al. (2019). Group S has a strong tendency to contain Tc-poor stars.

Table 3. Data of M-type Miras with $^{12}C/^{13}C \gtrsim 25$.

GCVS	Bumps	Tc	$^{12}C/^{13}C$
R Aur	yes	yes (3)	33±13
TX Cam	yes	–	21±6
T Cas	yes	yes (3)	33±5
T Cep	yes	yes (1)	33±10
U Her	yes	no (3)	19±8
RU Her	yes	yes (1)	25±5
R Hya	yes	yes (1)	26±4
S Ori	yes	yes (1)	45±13
U Ori	yes	poss (2)	25±10

Notes. Literature sources of Tc content: (1) Uttenthaler et al. (2019); (2) Little et al. (1987); (3) Uttenthaler et al. (in prep.)

the $K - [22]$ dust mass-loss indicator as a function of relative period change $\Delta P/\langle P\rangle$. All sample stars except the CPC and SPC Miras are plotted in this diagram in Fig. 10. Up to a level of $\Delta P/\langle P\rangle \sim 5\%$, the stars show a considerable spread in $K-[22]$ independent of spectral type, except for the S-type stars, which have several specimens with a lower colour index than the rest. Furthermore, we can identify a 'tail' of stars with more strongly varying periods. This group has two remarkable properties: (i) its colour indices are confined to the narrow range of $1.0 \lesssim K - [22] \lesssim 2.5$, and (ii) implying a limit of $\Delta P/\langle P\rangle \geq 5\%$, it is exclusively made up of M-type stars; these are the 18 MPC stars listed in Table 1. This feature led us to define the limit of 'significant period change' used throughout this paper; it suggests that the limit of $\Delta P/\langle P\rangle \geq 5\%$ is suitable to distinguish between random period variations known to occur in Mira stars (Templeton et al. 2005) and actual period changes. Stars that change period more than this could form a homogeneous group of MPC stars.

4.2. Mass loss from stars with significant period change

We inspect the $K - [22]$ colour of the 27 stars with significant period changes from Table 1 as a function of the mean period in Fig. 11. The stars do not appear to have particularly strong dust

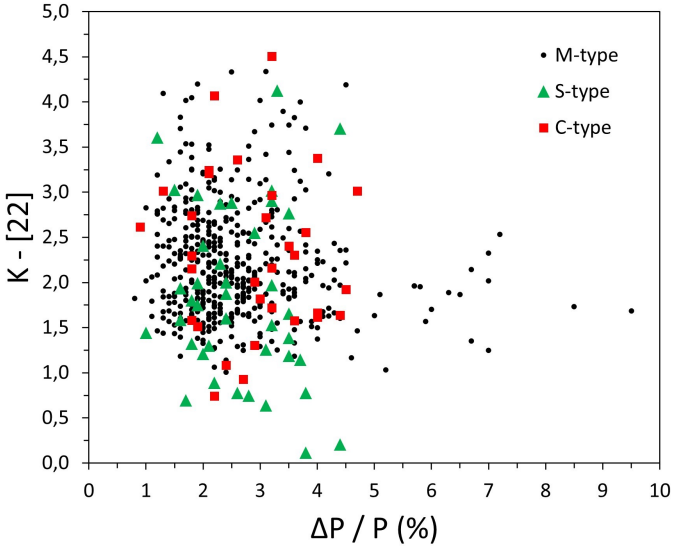

Fig. 10. $K - [22]$ vs. $\Delta P/\langle P\rangle$ diagram of our sample stars, excluding the SPC and CPC stars identified in Sect. 3.1. The chemical spectral types are distinguished by the symbols; see the legend. A few S stars have very low $K - [22]$ colours (dust mass-loss rate), and the 'tail' of more strongly varying periods (>5%) is exclusively made up of M stars.

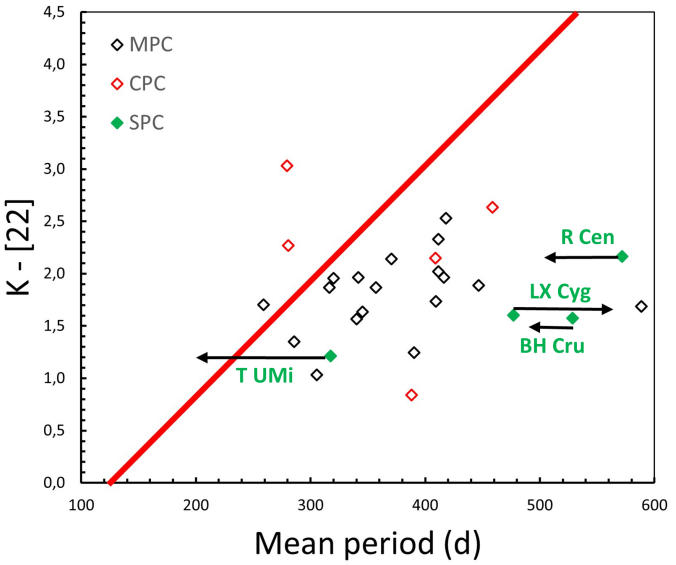

Fig. 11. $K - [22]$ vs. P diagram of the 27 stars in Table 1; see the legend for the identification of the three types of period change. The red solid line is the relation that best separates Tc-poor from Tc-rich Miras following Eq. (1). The arrows attached to the symbols of the SPC stars indicate their recent period evolution.

production, given that Miras can easily have $K - [22]$ colours above $4\overset{m}{.}0$ (Fig. 10). Uttenthaler et al. (2019) used this colour to study the mass loss from Miras with and without the 3DUP indicator Tc. These authors demonstrated that Tc-poor and Tc-rich stars occupy two distinct regions in the $K - [22]$ versus P diagram. The optimised linear relation that best separates the two groups takes the form:

$$K - [22] = 0.011 \times P - 1.380. \quad (1)$$

Tc-poor Miras are generally found above this line, whereas Tc-rich (post-3DUP) Miras are located below. This linear

relation is included in Fig. 11 to guide the eye. The accuracy of the separation was found to be 0.87, that is, the probability that a star is placed on the 'correct' side, according to its Tc content, is 87%. The location of a star in the $K-[22]$ diagram is therefore a strong indicator of the star having undergone TP events and subsequent 3DUP.

As already indicated by Fig. 10, stars with significant MPCs appear to have relatively low $K-[22]$ colours, or low dust mass-loss rates. Indeed, 17 out of 18 (94%) MPC stars are located below this separating line, where the 3DUP indicator Tc is usually detected. Only one star, S Sex, is located above the line, and by a narrow margin. This star has also been proposed as a candidate for having undergone a TP recently because of its substantial period decrease (Merchán Benítez & Jurado Vargas 2000). The location of the stars in this period–colour diagram supports the notion from Sect. 3.4 that the MPC phenomenon could be related to TP and subsequent 3DUP events.

In Fig. 11, we can also observe how the stars classified as SPCs all fall in the Tc-rich zone. This would be expected because a recent TP or 3DUP event has been proposed to cause the sudden period change. SPC stars are characterised by period changes that can be as large as ∼40% within a few decades, and so their location in the $K-[22]$ versus P diagram will present some uncertainties depending on the mean period used. For example, looking only at its Mira phase, the period change in T UMi amounts to 38%. We note that this star has recently switched from the fundamental Mira pulsation mode to a higher-overtone mode (Molnár et al. 2019). In Fig. 11, we indicated the period evolution by arrows. (We note that the colour might also have changed, but there are insufficient IR data to quantify this.) LX Cyg and BH Cru are C-type Miras, and so their location in the Tc-rich zone is consistent with expectations. For the latter, the arrow in Fig. 11 indicates the 9.5% period decrease since 1999.

On the other hand, the location of R Cen and T UMi in the $K-[22]$ versus P diagram is not consistent with the proposed separation of Tc-poor and Tc-rich Miras. Both stars are M-type and Tc-poor but located in the Tc-rich zone of the diagram. R Cen is a candidate for being a fairly massive star undergoing HBB. The ^{22}Ne neutron source operating in such stars produces only little Tc, and 3DUP events are inefficient, meaning that Tc is sufficiently enriched in the atmosphere only until after many TPs (García-Hernández et al. 2013). Reconstructing the $K-[22]$ infrared excess from historical observations, McDonald et al. (2020) showed that T UMi has become significantly less dusty since about 1975. It may well have been located in the Tc-poor region before the sudden period decrease commenced.

In any case, keeping in mind the different spectral types and directions of period evolution, even from these few stars, it is clear that the SPC group appears to be inhomogeneous, and that the observed period changes may reflect different physical processes going on in these stars (TPs, 3DUP). Also, the five CPC stars exhibit some diversity: three of them are located in the Tc-rich zone (R Hya, Z Tau, T Lyn) and two in the Tc-poor zone (W Dra, R Aql) in Fig. 11. The three CPC stars for which the Tc content is known (Table 2) are located in the part of the $K-[22]$ versus. P diagram expected for their Tc content. Also, the spectral types are diverse; see Table 1. We reiterate that the absence of Tc or ^{12}C enrichment does not necessarily mean that TPs are absent in those stars.

The assignment of the Tc-rich area in the $K-[22]$ versus. period diagram can be reviewed by inspecting the location of the 43 S-type and 33 C-type sample Miras in such a diagram. These stars are expected to have evolved to their current stage of carbon enrichment by repeated dredge-up of carbon and s-process elements (e.g., Tc). Figure 12 shows this diagram. The separation line defined by Eq. (1) is again included in this plot. It can be seen that 39/43 (91%) of the S-type and 27/33 (82%) of the C-type stars are located in the zone expected for Tc-rich stars. Some of the stars above the separating line are there only by a narrow margin. We remind the reader that Mira stars also have a non-negligible pulsation amplitude in the K-band and the measurements are often single-epoch observations. Thus, this selection of stars confirms the assignment of the region below Eq. (1) to Tc-rich, post-3DUP Miras.

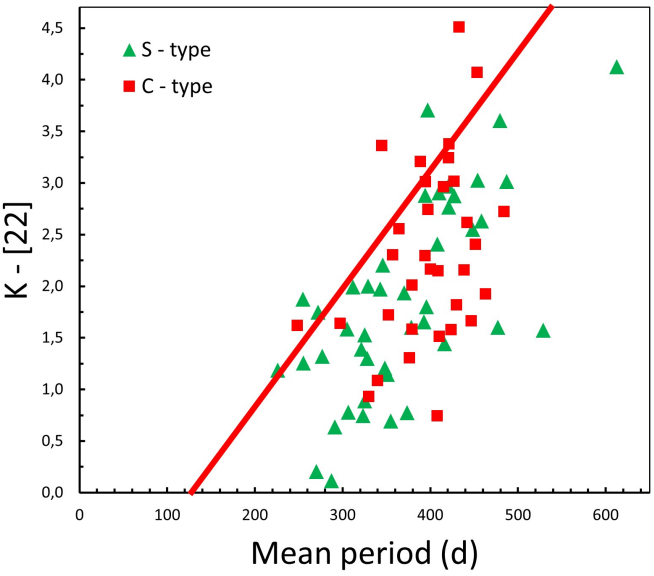

Fig. 12. $K-[22]$ vs. P diagram of the S- and C-type Miras in the sample. The red solid line is the relation that best separates Tc-poor from Tc-rich Miras according to Eq. (1). As expected, most of the stars are located in the area where Tc-rich Miras are found, i.e. below the line.

4.3. Mass loss and light-curve asymmetries

Separate $K-[22]$ versus P diagrams for Groups A and S are shown in Fig. 13. We note the different distributions in period: While Group A has a mean period of 378 d and starts to be populated at $P \gtrsim 240$ d, Group S has a mean period of 266 d and is mostly limited to $P \lesssim 400$ d. From the results regarding Tc in Sect. 3.4, it may be expected that many Group A stars are located below the separation line defined by Eq. (1), whereas Group S stars are above it. Indeed, 92% of the 203 Group A stars are located below the separation line. The few stars above the line are relatively close to it. Moreover, this fraction is almost insensitive to the spectral type: ∼94% M-type, ∼91% S-type, and ∼79% of the C-type Miras with bumps are located below the line given by Eq. (1).

The lower panel of Fig. 13 shows the $K-[22]$ versus P diagram of the 336 Group S stars. We note that this group is probably not as pure as Group A. Nevertheless, we can observe that the stars in Group S are mainly located above the line (∼89%) and seem to 'avoid' the zone below it. This percentage rises to 94% if we consider only the M-type stars. Many of the stars below the line are S- or C-type Miras that in turn have $K-[22]$ colours higher than their siblings at similar periods in Group A.

Figure 13 suggests that the same line Uttenthaler et al. (2019) found to separate Tc-rich from Tc-poor Miras also seems to separate stars with bumps in their light curves from those

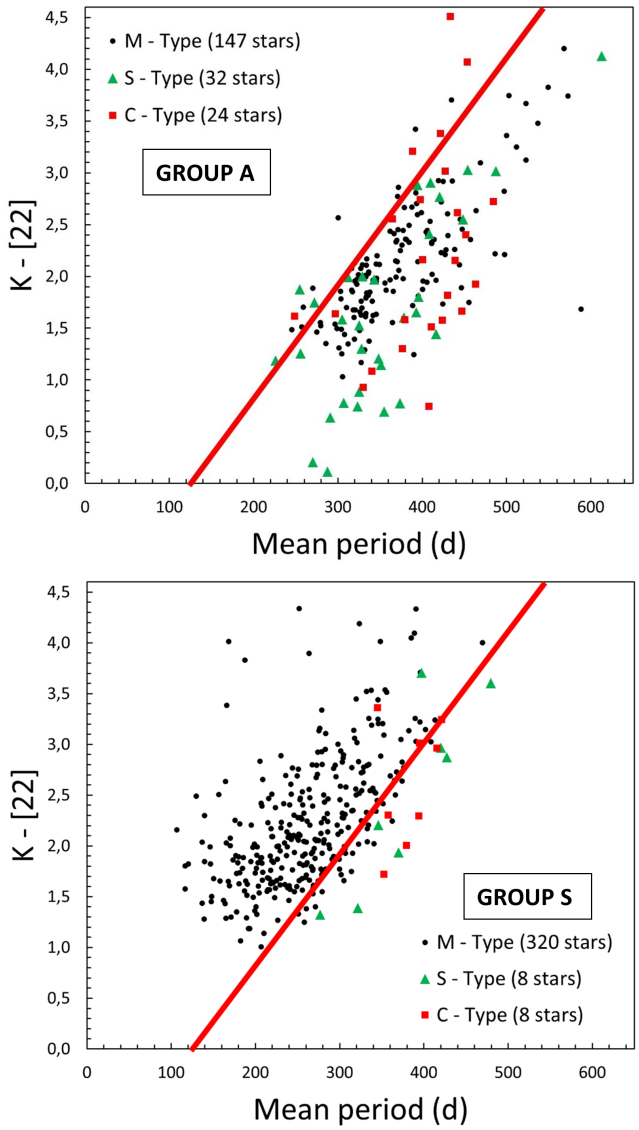

Fig. 13. $K-[22]$ vs. P diagram of Miras. *Upper panel:* Group A, with bumps or asymmetries in the ascending branch of their light curve. *Lower panel:* Group S, with symmetric light curves. The symbols distinguish the three main spectral types; see the legend. The solid red line is the linear relation given by Eq. (1). Evidently, Miras without bumps have higher $K-[22]$ colours (dust mass-loss rates) than their siblings with bumps at similar pulsation periods.

without. Surprisingly, stars with Tc in their spectra occupy the same region in the $K-[22]$ versus P diagram as stars with bumps in their light curves, as do stars without Tc and bumps. This suggests an association between 3DUP and the occurrence of bumps in the light curve of a Mira. One would not expect such a relation from theoretical considerations or previous observational results.

Instead of the K-band magnitude, we can also use the WISE [3.4] band, which has a central wavelength of ~3.4 μm. Advantages of the [3.4]- over the K band are that it was measured simultaneously with the [22] band and the variability amplitude is lower. Both should reduce the variability scatter in the colour index. The disadvantage is that bright Miras saturate some detector pixels in the [3.4] band, decreasing the accuracy for those stars. For stars that are not excessively dusty, the [3.4] band is still dominated by photometric emission, and we can establish the [3.4]−[22] colour as an indicator of dust mass-

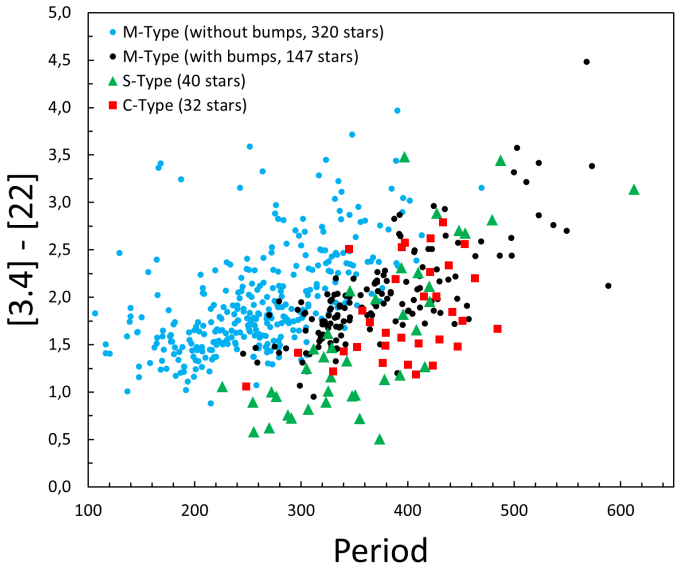

Fig. 14. [3.4]−[22] vs. P diagram of M-type Miras with and without light-curve bumps, respectively, as well as S- and C-type Miras.

loss rate. Figure 14 shows a [3.4]−[22] versus P diagram of our sample stars, distinguished by their symbols into M-type stars with bumps (Group A), M-type stars without bumps (Group S), S-type, and C-type stars. Again, this diagram clearly demonstrates the separation of the stars into different regions: M-type stars without bumps have higher [3.4]−[22] colours, that is, higher dust mass-loss rates, than other stars at similar periods. We note the location of a group of S-type stars at very low [3.4]−[22] colours that have barely any dust in their circumstellar envelopes.

5. Discussion

The new evidence from our sample allows us to draw conclusions as to the origin of significant MPCs. The Fourier spectra of MPC Miras show no prominent additional peaks beyond those corresponding to the harmonics of the primary frequency. This suggests that hypotheses invoking additional pulsation modes, such as those found to be acting in RV Tau stars (Buchler et al. 1996), disagree with the evidence collected here.

Following theoretical evolutionary models, Miras with significant MPCs could have a place in the interpulse period of the TP-AGB. TPs repeat quasi-periodically every few 10^4 yr, depending on stellar mass (e.g., Schwarzschild & Härm 1967; Wood & Zarro 1981). After an initial luminosity drop at the onset of a TP, the star is predicted to be more luminous than before the He-shell flash for a few hundred years. Stars with SPC (e.g., T UMi) and CPC (e.g., R Hya) have been suggested to currently pass through this phase (e.g., Wood & Zarro 1981; Uttenthaler et al. 2011). Subsequently, in a phase of a few thousand years at most, the He-burning shell is gradually extinguished, causing a decrease in luminosity below the level prior to the TP. In this sense, a possible interpretation for the observations could be that the large structural changes in the star between about 10^2 and 10^3 yr after the TP could be the origin of the significant MPCs, after which the pulsation period will regain stability as the stellar structure is restored. These shorter-period variations may be thermal relaxation oscillations in the stellar envelope, with Kelvin-Helmholtz cooling timescales (Ostlie & Cox 1986, $\tau_{KH} \sim 6-200$ yr) that broadly

coincide with the timescales of period variations found in MPC stars (~30−75 yr).

If significant MPCs have their origin in the aftermath of a TP, their number fraction (18/548 ≈ 3.3%) should reflect the fraction of the TP cycle in which MPCs occur. At a typical Mira mass of 1.8 $M_{\odot}$, state-of-the-art AGB evolutionary models (Marigo et al. 2013) predict an interpulse period of ~1.2×10^5 yr. This would mean that the star typically undergoes significant MPCs for ~4000 yr. We note that this is about half the time it takes the model star to reach the luminosity minimum after the onset of a TP. Indeed, several of the MPC stars in our sample have Tc lines in their spectra, meaning they must have undergone TPs in the past (Sect. 3.4). However, the puzzling piece of information is that the MPC group is made up exclusively of M-type Miras. Certainly, S- and C-type Miras also undergo TPs; the absence of significant MPCs among them is therefore unexpected. Given the distribution of chemical spectral types in our sample, the probability for this selection is 6.6%, which is low, but not low enough to conclude that it is not a chance result. A still larger sample of Miras, including more of type S and C, would be required to test this conclusion.

As a very high fraction (16/18) of the MPC Miras also have bumps on the ascending branch of their light curves, we inspected the light curves of all sample stars for asymmetries and divided them into two, Groups A (asymmetric) and S (symmetric). We confirm the conclusion made by Lebzelter (2011) that the fraction of light curves with asymmetries is much higher among S- and C-type Miras. Further evidence that the light-curve shape could be related to 3DUP events comes from the distribution of Tc in the M-type Miras in Groups A and S: while in Group A, they uniformly distribute between having Tc (post-3DUP) and not having Tc, almost all with symmetric light curves are devoid of Tc.

We also find evidence that MPC stars have reduced dust mass-loss rates. In a $K-[22]$ versus P diagram (Fig. 11), all MPC stars are located at relatively low values of the $K-[22]$ colour. In addition, through a diagram plotting $K-[22]$ or $[3.4]-[22]$ versus P (see Figs. 13 and 14), we demonstrate that stars with bumps have a decreased dust mass-loss rate compared to Miras with symmetric light curves at similar periods. No further relation between Mira light-curve shape and other stellar parameters is known to date.

The question remains as to how all these things are related. We still do not know why Miras with Tc, meandering period changes, and bumps in their light curves all fall in the same region of the $K-[22]$ versus P diagram, or why they have reduced $K-[22]$ colours (dust mass-loss rates) compared to Miras at similar periods but without either of these properties.

Uttenthaler et al. (2019) suggested that 3DUP, possibly through the dredge-up of radioactive isotopes, leads to reduced dust formation in the stellar envelope. Ions created upon the radioactive decay of unstable (*s*-process) isotopes could inhibit dust formation. In this way, reduced $K-[22]$, as an indicator of dust mass-loss rate, would also be connected to the occurrence of TPs that drive 3DUP. As discussed above, MPCs could also be related to a recent TP via a readjustment of the envelope structure. The fact that most of the MPC Miras, in addition to having a reduced $K-[22]$, also show Tc in their spectra supports the notion that they are in the TP-AGB phase. However, additional observations are required to strengthen the case.

Finally, the relation between light-curve asymmetries and this aggregate of phenomena has yet to be established. Liljegren et al. (2016, 2017), using numerical experiments with dynamic Mira model atmospheres, showed that the wind properties of a mass-losing model are susceptible to the luminosity and radius evolution during a pulsation cycle because of the importance of the timing between dust formation and radiation pressure. Deviations from a sinusoidal light curve might have a detrimental effect on the mass-loss rate. If dust formation in the stellar envelope is hindered by the effects of 3DUP (i.e. radioactive decay of unstable isotopes), this could affect the light-curve shape. Suppose the dust is formed inefficiently in the wake of an outwardly propagating shock wave, or it couples less efficiently to the radiation pressure from the central star. In this case, significant dust amounts would fall back towards the star instead of being accelerated outwards. The infalling material would hit the outwardly moving shock wave of the next pulsation cycle, causing bumps or secondary maxima in the light curve. In this way, bumps in the light curves may be connected to the occurrence of 3DUP, and the stars might end up at a reduced $K-[22]$ colour exactly where Tc-rich post-3DUP Miras are located.

6. Summary and conclusions

We collected long-term light curves of 548 Miras in the solar neighbourhood from several databases (AAVSO, AFOEV, ASAS, and DASCH) and analysed them for period changes and variations over timescales of several decades. In total, we identify 27 Miras with relative period changes in excess of 5%. We confirm all identifications of period-changing stars from earlier studies (Templeton et al. 2005) and add one more star with a continuously decreasing pulsation period, T Lyn. The period of this carbon star has decreased by 6.4% over the past ~80 yr. For BH Cru, a star that was previously reported to have undergone a sudden period increase by ~25% before 1999, we find that since then the period has decreased again by ~9%. Eighteen stars exhibit significant meandering period changes (MPCs) with relative period changes $\Delta P/P \geq 5.0\%$, all of which are of spectral type M. This MPC group is also characterised by a relatively low mid-IR excess. Furthermore, we find that the median (random) period change of Miras is ~2.4%, which should also be the accuracy with which periods can be determined from long-term light curves.

As we noticed that MPC Miras show asymmetries (bumps) in their light curves, we extended our analysis to light curve shapes of the stars. The sample was divided into two groups, one with bumps or other anomalies in their light curves (203/548 ≈ 37%), and those seemingly without such asymmetries (336/548 ≈ 63%). Our sample clearly confirms the suggestion found by Lebzelter (2011) that S- and C-type Miras are strongly over-represented in the group with asymmetric light curves. We searched for further stellar parameters that distinguish these two groups and find that they clearly locate in two different regions of a $K-[22]$ versus P diagram in the sense that, at a given pulsation period, Miras without bumps have higher $K-[22]$ colour (dust mass-loss rate) than those with bumps. No such distinction was reported previously.

Our empirical results are both clear and intriguing. We speculate that the origin of MPCs lies in thermal oscillations of the stellar envelope in the aftermath of a thermal pulse because of the similarity of observed and predicted timescales and the stars' 3DUP activity. However, the fact that MPC Miras in our sample are exclusive of M-type is puzzling. Furthermore, the co-location in a $K-[22]$ versus P diagram of Miras that can be distinguished by seemingly unconnected characteristics is surprising. At a given pulsation period, Miras with significant period changes or bumps in their light curves have distinctively lower $K-[22]$ colours (dust mass-loss rates) than Miras without. The

same is true for Miras with 3DUP activity, as indicated by the presence of Tc in their spectra and increased ^{12}C abundance compared to Miras without 3DUP. We speculate that all of these relationships could be linked to the occurrence of TPs and 3DUP events, but better and more targeted data are needed to test this hypothesis.

Acknowledgements. We acknowledge with thanks the variable star observations from the AAVSO International Database contributed by observers worldwide and used in this research. This publication makes use of data products from the Two Micron All Sky Survey, which is a joint project of the University of Massachusetts and the Infrared Processing and Analysis Center/California Institute of Technology, funded by the National Aeronautics and Space Administration and the National Science Foundation. This publication makes use of data products from the Wide-field Infrared Survey Explorer, which is a joint project of the University of California, Los Angeles, and the Jet Propulsion Laboratory/California Institute of Technology, funded by the National Aeronautics and Space Administration. This publication make use of light curves from the ASAS-SN project, specifically from the ASAS-SN Catalog of Variable Stars III. The DASCH project at Harvard is partially supported by NSF grants AST-0407380, AST-0909073, and AST-1313370.

References

Abia, C., & Isern, J. 1997, MNRAS, 289, L11
Buchler, J. R., Kollath, Z., Serre, T., & Mattei, J. 1996, ApJ, 462, 489
Campbell, L. 1925, Harvard Reprint, No. 21
Cutri, R. M., Wright, E. L., Conrow, T., et al. 2021, VizieR Online Data Catalog, II/328
Dominy, J. F., & Wallerstein, G. 1987, ApJ, 317, 810
Foster, G. 1996, AJ, 112, 1709
Gal, J., & Szatmary, K. 1995, A&A, 297, 461
García-Hernández, D. A., Zamora, O., Yagüe, A., et al. 2013, A&A, 555, L3
Greaves, J. S., & Holland, W. S. 1997, A&A, 327, 342
Hawkins, G., Mattei, J. A., & Foster, G. 2001, PASP, 113, 501
Herwig, F. 2005, ARA&A, 43, 435
Hinkle, K. H., Lebzelter, T., & Straniero, O. 2016, ApJ, 825, 38
Jayasinghe, T., Stanek, K. Z., Kochanek, C. S., et al. 2019, MNRAS, 485, 961
Kiss, L. L., & Szatmáry, K. 2002, A&A, 390, 585
Kiss, L. L., Szatmáry, K., Cadmus, R. R. Jr., & Mattei, J. A. 1999, A&A, 346, 542
Lambert, D. L., Gustafsson, B., Eriksson, K., & Hinkle, K. H. 1986, ApJS, 62, 373
Laycock, S., Tang, S., Grindlay, J., et al. 2010, AJ, 140, 1062
Lebzelter, T. 2011, Astron. Nachr., 332, 140
Lebzelter, T., Hinkle, K. H., Straniero, O., et al. 2019, ApJ, 886, 117
Liljegren, S., Höfner, S., Nowotny, W., & Eriksson, K. 2016, A&A, 589, A130
Liljegren, S., Höfner, S., Eriksson, K., & Nowotny, W. 2017, A&A, 606, A6
Little, S. J., Little-Marenin, I. R., & Bauer, W. H. 1987, AJ, 94, 981
Lockwood, G. W., & Wing, R. F. 1971, ApJ, 169, 63
Ludendorff, H. 1928, Handbuch der Astrophysik (Berlin: Verlag Von J. Springer), 6, 49
Marigo, P., Bressan, A., Nanni, A., Girardi, L., & Pumo, M. L. 2013, MNRAS, 434, 488
McDonald, I., De Beck, E., Zijlstra, A. A., & Lagadec, E. 2018, MNRAS, 481, 4984
McDonald, I., Uttenthaler, S., Zijlstra, A. A., Richards, A. M. S., & Lagadec, E. 2020, MNRAS, 491, 1174
Merchán Benítez, P., & Jurado Vargas, M. 2000, A&A, 353, 264
Merchán Benítez, P., & Jurado Vargas, M. 2002, A&A, 386, 244
Molnár, L., Joyce, M., & Kiss, L. L. 2019, ApJ, 879, 62
Ohnaka, K., & Tsuji, T. 1996, A&A, 310, 933
Ostlie, D. A., & Cox, A. N. 1986, ApJ, 311, 864
Percy, J. R. 2015, JAAVSO, 43, 223
Ramstedt, S., & Olofsson, H. 2014, A&A, 566, A145
Samus', N. N., Kazarovets, E. V., Durlevich, O. V., Kireeva, N. N., & Pastukhova, E. N. 2017, Astron. Rep., 61, 80
Schlafly, E. F., Meisner, A. M., & Green, G. M. 2019, ApJS, 240, 30
Schöier, F. L., & Olofsson, H. 2000, A&A, 359, 586
Schwarzschild, M., & Härm, R. 1967, ApJ, 150, 961
Shappee, B. J., Prieto, J. L., Grupe, D., et al. 2014, ApJ, 788, 48
Skrutskie, M. F., Cutri, R. M., Stiening, R., et al. 2006, AJ, 131, 1163
Soszynski, I., Dziembowski, W. A., Udalski, A., et al. 2007, Acta Astron., 57, 201
Templeton, M. R., Mattei, J. A., & Willson, L. A. 2005, AJ, 130, 776
Uttenthaler, S., van Stiphout, K., Voet, K., et al. 2011, A&A, 531, A88
Uttenthaler, S., Greimel, R., & Templeton, M. 2016a, Astron. Nachr., 337, 293
Uttenthaler, S., Meingast, S., Lebzelter, T., et al. 2016b, A&A, 585, A145
Uttenthaler, S., McDonald, I., Bernhard, K., Cristallo, S., & Gobrecht, D. 2019, A&A, 622, A120
Vanture, A. D., Smith, V. V., Lutz, J., et al. 2007, PASP, 119, 147
Vardya, M. S. 1988, A&AS, 73, 181
Whitelock, P. A. 1999, New A Rev., 43, 437
Wood, P. R., & Zarro, D. M. 1981, ApJ, 247, 247
Wright, E. L., Eisenhardt, P. R. M., Mainzer, A. K., et al. 2010, AJ, 140, 1868
Ya'Ari, A., & Tuchman, Y. 1996, ApJ, 456, 350
Zijlstra, A. A., & Bedding, T. R. 2002, JAAVSO, 31, 2
Zijlstra, A. A., Bedding, T. R., & Mattei, J. A. 2002, MNRAS, 334, 498

Appendix A: Additional figure

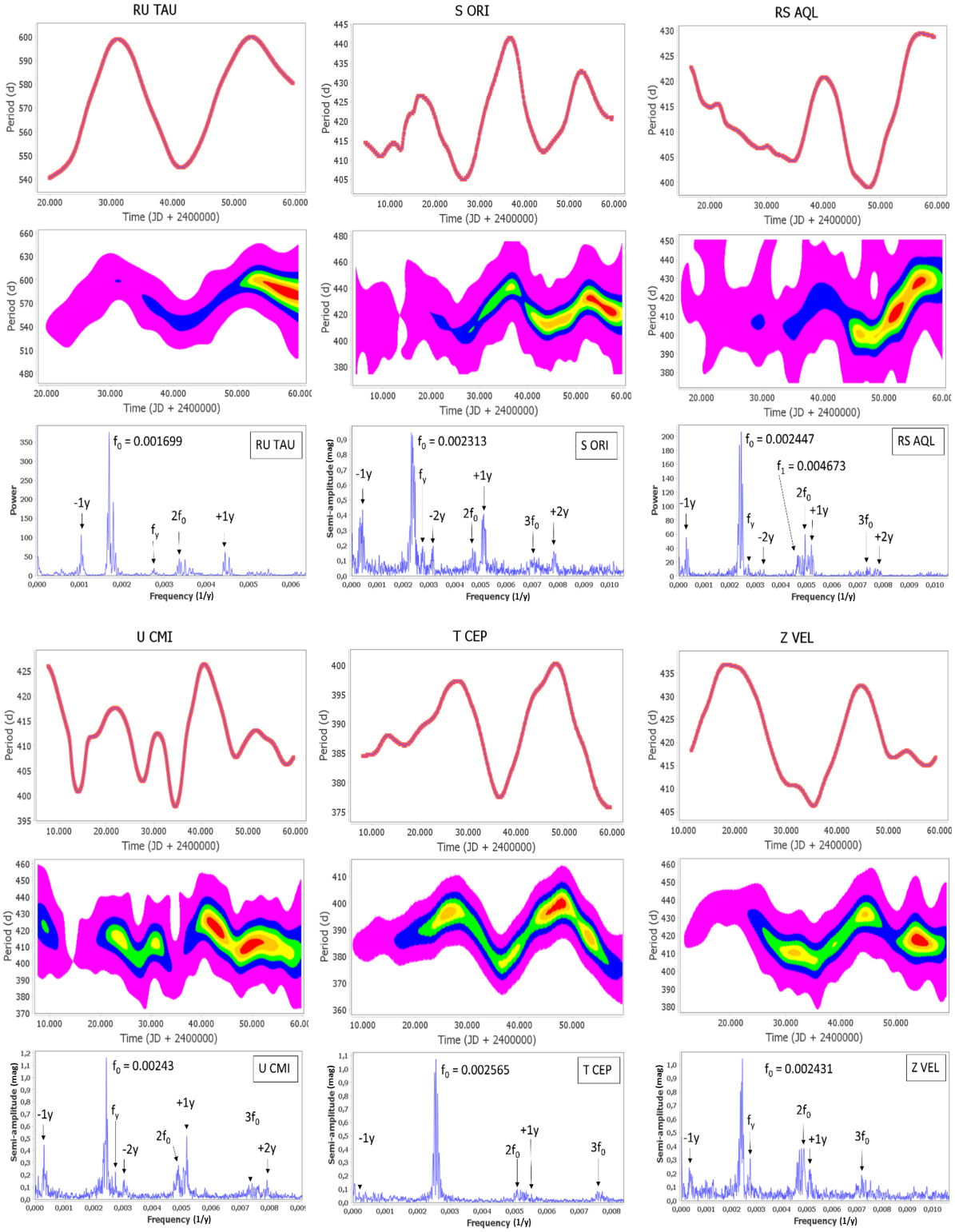

Fig. A.1. Period as a function of time and WWZ, Fourier spectra, and identification of the relevant peaks for the 18 stars with significant MPCs. From left to right and from top to bottom, the stars are arranged in decreasing order of $\Delta P/\langle P \rangle$.

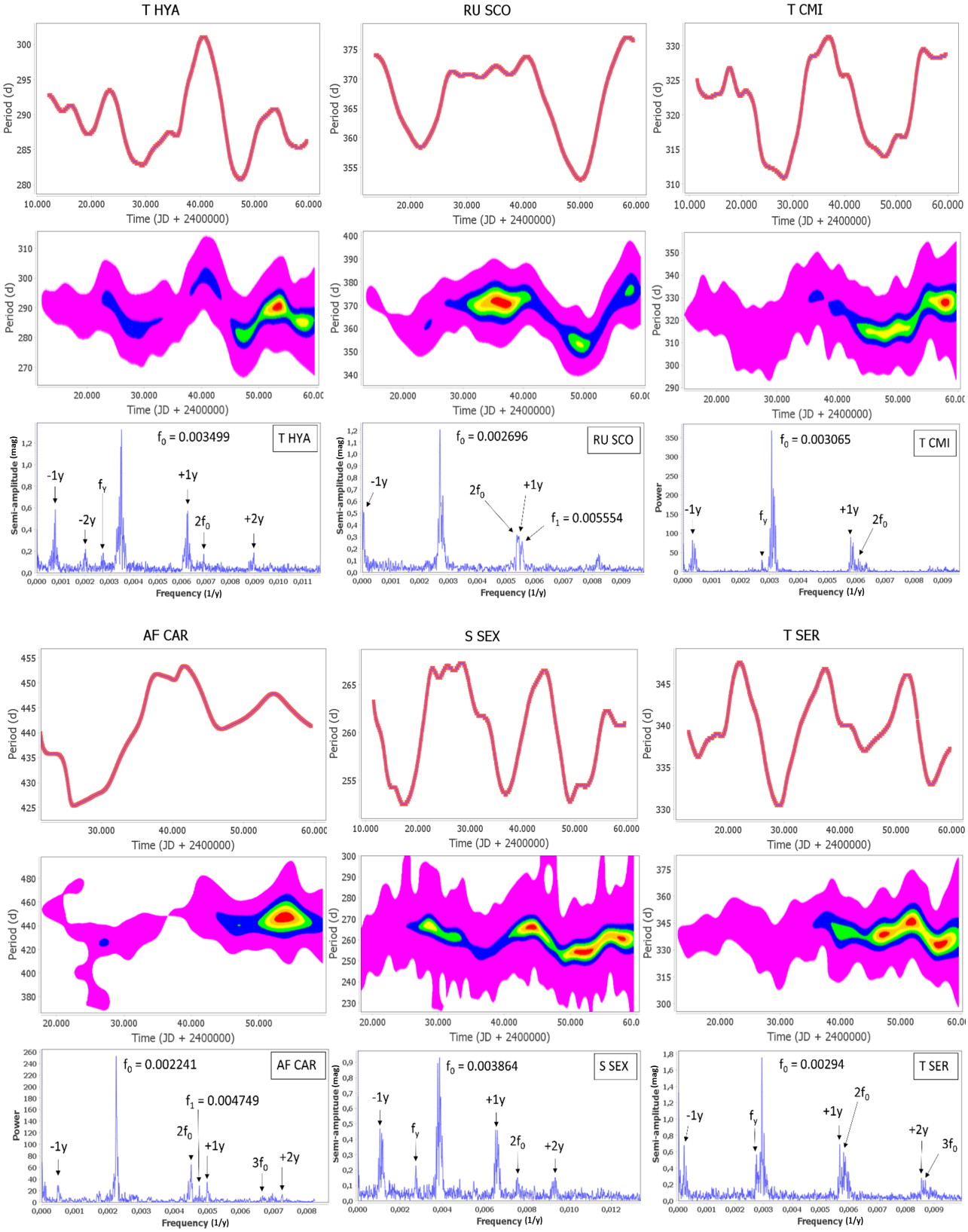

Fig. A.1. continued.

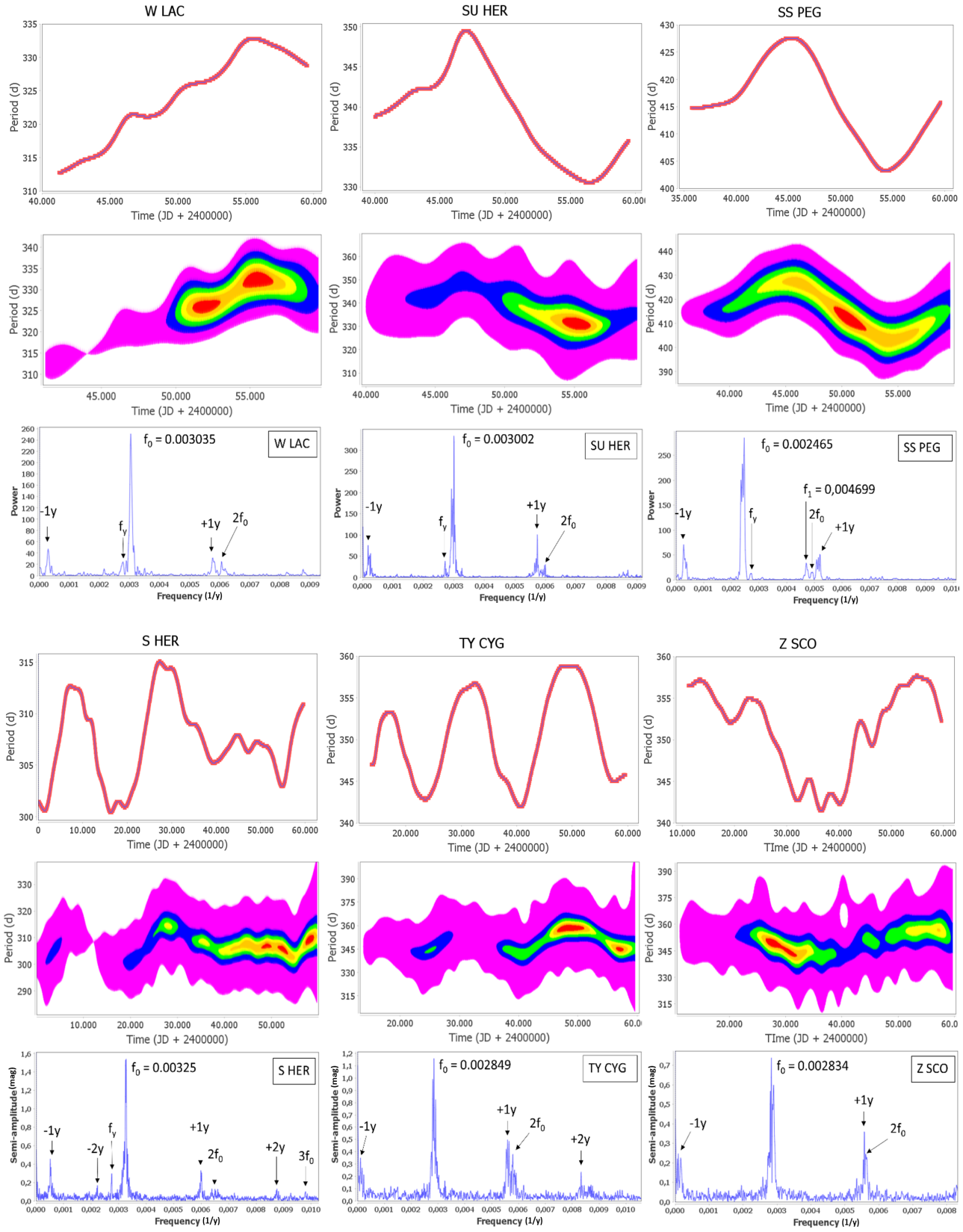

Fig. A.1. continued.

Appendix B: Additional table

Table B.1. Data of the 548 sample Mira stars.

GCVS	S.Type	Period	$\Delta P/P$	Bumps	Tc	$^{12}C/^{13}C$	$K-[22]$	[3.4]–[22]
AK And	S:	321.3	3.5	0			1.388	1.371
AZ And	M4	195.2	3.1	0			2.206	1.549
BG And	S6.5.5e	291.0	3.1	1			0.636	0.727
BU And	M7e	380.4	4.5	1			2.359	2.173
R And	S3.5e-S8.8e(M7e)	410.0	3.2	1	yes[a]	40 ± 15[1]	2.905	2.259
RR And	S6.5.2e	327.9	2.1	1			1.300	1.162
RW And	M5e-M10e(S6.2e)	429.9	2.3	1			2.602	2.166
RY And	M8	392.5	1.8	1			2.807	2.867
SV And	M5e-M7e	315.3	3.5	0			1.926	2.014
SX And	M6.5e	332.7	2.4	1			1.612	1.325

Notes. Meaning of Column 5: 0: Stars with symmetric light curves (Group S); 1: Stars with asymmetric light curves (Group A). Literature sources of Tc content in Column 6: (a) Uttenthaler et al. (2019); (b) Little et al. (1987); (c) Uttenthaler et al., in preparation; (d) Vanture et al. (2007). Literature sources of $^{12}C/^{13}C$ content in Column 7: (1) Hinkle et al. (2016); (2) Ramstedt & Olofsson (2014); (3) Ohnaka & Tsuji (1996); (4) Abia & Isern (1997); (5) Lebzelter et al. (2019); (6) Schöier & Olofsson (2000); (7) Dominy & Wallerstein (1987). The full table is available a the CDS.